Effect of volume growth on the percolation threshold in random directed acyclic graphs with a given degree distribution

Schamboeck, V.; Kryven, I.; Iedema, P.D.

DOI
10.1103/PhysRevE.101.012303

Publication date
2020

Document Version
Final published version

Published in
Physical Review E

Effect of volume growth on the percolation threshold in random directed acyclic graphs with a given degree distribution

Verena Schamboeck [1,*] Ivan Kryven [2] and Piet D. Iedema [1]

[1] *Van 't Hoff Institute for Molecular Sciences, University of Amsterdam, Science Park 904, 1098 XH Amsterdam, Netherlands*

[2] *Mathematical Institute, Utrecht University, PO Box 80010, 3508 TA Utrecht, Netherlands*

(Received 19 June 2019; published 14 January 2020)

In every network, a distance between a pair of nodes can be defined as the length of the shortest path connecting these nodes, and therefore one may speak of a ball, its volume, and how it grows as a function of the radius. Spatial networks tend to feature peculiar volume scaling functions, as well as other topological features, including clustering, degree-degree correlation, clique complexes, and heterogeneity. Here we investigate a nongeometric random graph with a given degree distribution and an additional constraint on the volume scaling function. We show that such structures fall into the category of m-colored random graphs and study the percolation transition by using this theory. We prove that for a given degree distribution the percolation threshold for weakly connected components is not affected by the volume growth function. Additionally, we show that the size of the giant component and the cyclomatic number are not affected by volume scaling. These findings may explain the surprisingly good performance of network models that neglect volume scaling. Even though this paper focuses on the implications of the volume growth, the model is generic and might lead to insights in the field of random directed acyclic graphs and their applications.

DOI: 10.1103/PhysRevE.101.012303

I. INTRODUCTION

In all networks one may attribute a notion of a distance to a pair of nodes, by taking the length of the shortest path connecting these nodes. One therefore may speak of a ball of radius r centered at a chosen node, where r is a positive integer. Studying how the expected volume of such a ball grows with r gives a good proxy characterizing the interplay of the space and structure of spatial random networks [1–5]: If this quantity has a simple monomial shape r^d, then one says that d is the network's dimension or volume scaling [3,4,6,7]. Dimensions of many real-life and artificial networks tend to range from approximately 1.25 for the New York City subway to 8.1 for YouTube [3]. The behavior becomes especially pronounced when the edge lengths are constrained as in, for instance, polymer networks [8], gels [9,10], and glasses [11,12]. In contrast, small-world networks [13] have volume scaling α^r and therefore do not feature a finite dimension.

Complex networks that are viewed within the context of their embedding space can be loosely defined as geometric graphs or spatial networks [14]. The information about embedding space might be given *a priori*, as in geometric graphs, or the space, that is to say, the network geometry, may be defined by the network's metric, thus emergent or hidden space [13,15–18]. Although spatial networks are ubiquitous in a geographic context (road [19], transportation [20], and river networks [21]), materials science (polymers [1], jammed glasses [11], rubber, and gels [10]), and biology (cell growth [22], cytoskeletons [23], and cellular and neural networks [24]), it is not clear how the metric induced by the network is related to the global properties of random networks. Thus, the underlying long-standing question, which is also topical in many other studies [25], is the following: Which topological constraints are necessary for a random graph model to reproduce the same global emergent properties as a given, possibly spatial, real-world network?

In this paper we focus on one emergent property in particular, namely, the percolation threshold [26]. The effect of the metric on the percolation threshold is difficult to assess as real-world spatial networks often feature a variety of properties that affect such a threshold, for instance, clustering, degree-degree correlation, and clique complexes [27]. However, neither clustering nor degree-degree correlation is a necessary property of spatial networks. Nevertheless, all spatial networks feature volume scaling that is in accordance with the underlying metric space. It is not clear whether spatial networks feature different percolation thresholds due to the their volume scaling or different thresholds appear due to other factors that tend to occur in, but not necessarily belong to, spatial networks.

The first attempts to develop a random network model where volume growth is fixed to a given function, characteristic of three-dimensional Euclidean space, appeared in polymer science [2,28], thus by requiring r^d scaling, $2 \leqslant d \leqslant 3$, in any polymer network irrespective of the network density. In other words, polymer networks are a very convincing example of real-life networks that are not small world. For decades, lattices were used in polymer network modeling due to their inherently correct volume growth. However, the downside of lattice models is their underlying periodic structure, which, on one hand, alters the percolation threshold and, on the

*v.schamboeck@uva.nl

other hand, forces periodicity onto the random structure of polymer networks. Polymer science has high expectations of the configuration model as the degree distributions of polymer networks are fully determined and limited by the underlying chemistry. The configuration model tends to be better and more efficient in explaining experimental observations of branched polymers than lattices [1,10,29,30]. However, the exponential volume growth associated with the conventional configuration model is a factor that convincingly shows the model's limitation [1], especially in networks that are far above their percolation threshold.

In this work we develop the null model for a maximum entropy network, or random graph, that has a layered structure and satisfies a given degree distribution. The fraction of nodes in every layer is defined by an arbitrary volume growth function, which we choose in accordance with the volume scaling in Euclidean d-dimensional space. The presented model can be thought of as a special case of a multilayer network [26], in which the number of layers tends to infinity and the fraction of nodes in each layer is fixed. In other words, the model characterizes an infinitely sized random directed acyclic graph with arbitrary degree distribution.

Directed acyclic graphs experience wide applications in citation networks [31,32], epidemiology [33,34], and food webs [35]. Many artificial networks feature a layered structure, where the number of nodes per layer is set by the design. Most notably, the design of (deep) neural networks often implies an inverse hourglass topology, which corresponds to a peculiar nonmonomial growth function that is also covered in this work.

In the rest of the paper we show how an infinite configuration model with colored edges [26,36] can be used to realize the model with controlled volume growth. This is done by constructing the colored degree distribution in such a way that its marginal corresponds to the desired degree distribution and the moments in each layer are given in accordance with the volume growth function. We then show that, surprisingly, when the degree distribution is fixed, the growth function has no effect on the percolation threshold. This result may shed light on one of the reasons why the Molloy-Reed criterion is so effective [37], even when applied to networks that the criterion is not originally designed for, i.e., spatial networks in this case.

II. MODEL

We introduce a network model with layered structure and the layers (generations) being connected in a consecutive manner. Nodes of generation g are only allowed to connect to nodes of generation $g-1$ and $g+1$. The degree distribution $u(k)$, which is the probability that a randomly chosen node has degree k, is arbitrary and fixed as a model parameter. In the present model, all nodes of the network satisfy the same degree distribution $u(k)$, independently of their associated generation. Let $n(g)$ be the fraction of nodes in generation g, which is the same as the probability that a node chosen uniformly at random is part of generation g. In the course of this section we will establish the precise relationship between the fraction of nodes per generation $n(g)$ and the arbitrary volume growth function $P(g)$, which allows us to design a network with arbitrary growth behavior of the fraction of nodes per generation. The only input to the model is the degree distribution $u(k)$, the volume growth function $P(g)$, and the total number of generations G. Apart from these constraints, the network is entirely random.

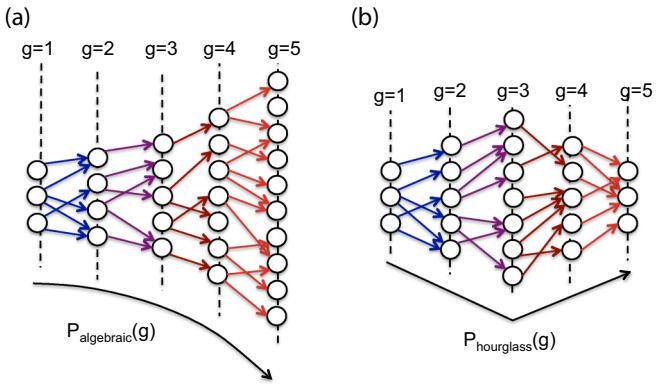

FIG. 1. Illustration of the generation model. The directed layered network is illustrated, with the edge orientation in accordance with the generation sequence. Networks with two different volume growth functions are shown: (a) monomial growth and (b) inverted hourglass.

The presence of the volume growth function $P(g)$ that defines the fraction of nodes in every generation is inspired by spatial networks. In spatial networks, the number of neighbors at generation g often grows in a similar manner as the volume of a ball in the corresponding metric space, where g is mapped to the radius of the ball. Figure 1 illustrates the concept of the generation model depicting two generation networks with different volume growth functions $P(g)$. Explicit examples of volume growth functions will be discussed in Sec. II B.

The model utilizes the following concept. The consecutive generations of the network are represented as a directed graph (see Fig. 1). The orientation of the directed edges is in accordance with the sequence of the consecutive generations, that is, the edges point from generation $g-1$ to generation g with $g = 1, \ldots, G$. Thus, the resulting network describes a directed acyclic graph. It is important to note that nodes exist that do not have in-edges, i.e., they may not be linked to the previous generation by a directed path but might be linked via an undirected path (a path irrespective of the orientation of the edges). Therefore, the network in general does not have one distinct root node. Since we differentiate in- and out-edges, degree k is split into the in-degree k_1 and out-degree k_2 with $k = k_1 + k_2$. A directed edge between generations is formed by pairing an out-edge of one generation with an in-edge of the consecutive generation.

Let the volume growth function $P(g)$ be the probability that a half-edge of a node in generation g is identified as an in-edge and $Q(g) = 1 - P(g)$ that it is an out-edge, always satisfying $P(g), Q(g) \geqslant 0$. We require the expected number of out-edges of generation g to be equal to the expected number of in-edges of generation $g+1$ for $g = 1, \ldots, G-1$. Under the assumption that the expected number of half-edges per node is the same in all generations, which is the case if all generations satisfy the same degree distribution, this requirement is

given by

$$[1 - P(g)]n(g) = P(g+1)n(g+1). \tag{1}$$

Therefore, we can write $n(g+1)$ as

$$n(g+1) = \frac{1 - P(g)}{P(g+1)} n(g), \tag{2}$$

with $n(1) = \frac{1}{N}$, where $N = 1 + \sum_{g=2}^{G} \prod_{i=1}^{g-1} \frac{1-P(i)}{P(i+1)}$ is the normalization factor. The number of nodes per generation $n(g)$ is thus related to the expected in- and out-degree in each generation. For example, under the assumption that nodes of all generations satisfy the same degree distribution and the expected in-degree is always smaller than the expected out-degree, then the fraction of nodes per generation increases with every generation. Note that in the general case, $P(g)$ is explicitly dependent on the generation g.

We define the ratio of nodes of consecutive generations as

$$x(g) = \frac{n(g+1)}{n(g)}. \tag{3}$$

In the case of monomial volume growth, $x(g)$ will monotonically decrease from $x(g) > 1$ to $x(g) \to 1$ for $g \to \infty$. If $x(g) \equiv \mathcal{C}$ and $\mathcal{C} > 1$, the expected number of nodes per generation increases exponentially.

Let the degree distribution $u(k)$ be arbitrary, however bounded by the maximum degree $F < \infty$ and normalized $\sum_{k=0}^{F} u(k) = 1$. The moments of the degree distribution are given by

$$\mu_n = \sum_{k=0}^{F} k^n u(k), \tag{4}$$

with μ_1 denoting the expected number of half-edges per node, i.e., the expected degree. Since the total number of half-edges of a node is randomly partitioned into in- and out-edges according to the probabilities $P(g)$ and $Q(g)$, the directed degree distribution $u^{[g]}(k_1, k_2)$ defining the probability that a node in generation g has k_1 in- and $k_2 = k - k_1$ out-edges is given by the binomial distribution

$$u^{[g]}(k_1, k_2) = \binom{k_1 + k_2}{k_1} P(g)^{k_1} Q(g)^{k_2} u(k_1 + k_2), \tag{5}$$

with $\sum_{k_1,k_2} u^{[g]}(k_1, k_2) = 1$. Let the partial moments of the degree distribution be defined as

$$\mu_{mn}^{[g]} = \sum_{k_1,k_2} k_1^m k_2^n u^{[g]}(k_1, k_2). \tag{6}$$

Substituting Eq. (5) into Eq. (6) leads to

$$\begin{aligned}
\mu_{10}^{[g]} &= \mu_{01}^{[g]} = \mu_1 P(g) = \mu_1 Q(g), \\
\mu_{11}^{[g]} &= (\mu_2 - \mu_1) P(g) Q(g), \\
\mu_{20}^{[g]} &= \mu_1 P(g) Q(g) + \mu_2 P(g)^2, \\
\mu_{02}^{[g]} &= \mu_1 P(g) Q(g) + \mu_2 Q(g)^2,
\end{aligned} \tag{7}$$

with $\mu_{10}^{[g]}$ the expected number of in-edges and $\mu_{01}^{[g]}$ the expected number of out-edges of a node of generation g.

A. Connection of the m-colored directed random graph to the generation model

The generation model can be formulated in terms of a random m-colored directed graph [26] as follows. Edges that connect two distinct generations are assigned one color. Generations are connected consecutively and the edge orientation is such that it points towards the higher generations. A half-edge type is then defined by color and direction (in- or out-edge). Thus, any node bears half-edges with at most two distinct colors: one color for in-edges that connect the node to the previous generation and one for the out-edges connecting the node with the next generations.

Instead of treating the first and last generations as special generations with only one type of edges, we allow them to have both in- and out-edges. Also, we define pairing between the out-edges of generation G and in-edges of generation 1. If desired, the probability of having in-edges in the first generation and out-edges in the last generations can be chosen to be zero by assigning $P(1) = 0$ and $P(G) = 1$ in the volume growth function. Another option is to allow the last generation to connect to the first generation, if $n(1)P(1) = n(G)[1 - P(G)]$ and $0 \leqslant P(g) \leqslant 1$ is satisfied. In this case any node features two half-edge types, including the first and last generations. This leads to the number of colors being G and the number of half-edge types being $2G$.

In order to formulate the network with generations as a special case of the directed m-colored random graph, we consider for every node a vector of half-edge counts $\mathbf{k} = (k_1, \ldots, k_{2g-1}, k_{2g}, \ldots, k_{2G})$ of all possible half-edge types where $g \in \{1, \ldots, G\}$. The presence of generations is then enforced by a strong constraint on the count vector: The count vector can only contain at most two nonzero elements, namely, k_{2g-1} and k_{2g}. The count k_{2g-1} is the in-degree and k_{2g} is the out-degree of nodes of generation g.

The permutation matrix $\boldsymbol{P}$ defines the pairing rules between half-edges. In the case of only one generation (color), we have

$$\boldsymbol{P}^{[1]} = \begin{pmatrix} 0 & 1 \\ 1 & 0 \end{pmatrix}. \tag{8}$$

A nonzero element $P_{i,j} = 1$ indicates that a half-edge of type i pairs with a half-edge of type j. In this case, out-edges are paired with in-edges and the other way around. In the case of G generations (and G colors), the $2G \times 2G$ permutation matrix is given by

$$\boldsymbol{P} = \begin{pmatrix}
0 & 0 & 0 & 0 & 0 & 1 \\
0 & \boldsymbol{P}^{[1]} & \mathbf{0} & \cdots & \mathbf{0} & 0 \\
0 & \mathbf{0} & \boldsymbol{P}^{[1]} & \ddots & \vdots & \vdots \\
\vdots & \vdots & \ddots & \ddots & \mathbf{0} & 0 \\
0 & \mathbf{0} & \cdots & \mathbf{0} & \boldsymbol{P}^{[1]} & 0 \\
1 & 0 & 0 & 0 & 0 & 0
\end{pmatrix}, \tag{9}$$

with $\boldsymbol{P}^{[1]}$ as defined in Eq. (8) and $\mathbf{0}$ being a 2×2 zero matrix.

The general expression for the elements of $\boldsymbol{M}$ is given by

$$\boldsymbol{M}_{i,j} = \frac{\mathbb{E}[k_i k_j]}{\mathbb{E}[k_j]} - \delta_{i,j}, \tag{10}$$

where expectation value $\mathbb{E}[f(\boldsymbol{k})]$ of a function $f(\boldsymbol{k})$ with respect to the degree distribution $u(\boldsymbol{k})$ is defined as

$$\mathbb{E}[f(\boldsymbol{k})] = \sum_{\boldsymbol{k}\geqslant 0} f(\boldsymbol{k})u(\boldsymbol{k}). \tag{11}$$

Thus, the expectation values $\mathbb{E}[k_j]$ and $\mathbb{E}[k_ik_j]$ in Eq. (11) are first and second moments of the count vector $\mathbf{k}$.

The probability that a randomly chosen node is part of generation g, that is, it has k_{2g-1} in- and k_{2g} out-edges, is given by

$$u(\mathbf{k}) = \begin{cases} n(g)u^{[g]}(k_{2g-1}, k_{2g}) & \text{for } k_{2g-1}, k_{2g} \geqslant 0; \\ & k_{2i-1}, k_{2i} = 0\ (i \neq g) \\ 0 & \text{otherwise,} \end{cases} \tag{12}$$

with $u^{[g]}(i, j)$ given in Eq. (5). Having the degree distribution of the whole system $u(\mathbf{k})$, the expected number of edges in each generation can be expressed as,

$$\begin{aligned} \mathbb{E}[k_{2g-1}] &= \mu_{10}^{[g]} n(g), \\ \mathbb{E}[k_{2g}] &= \mu_{01}^{[g]} n(g), \end{aligned} \tag{13}$$

where $\mu_{mn}^{[g]}$ is given in Eq. (6). The second-order expectation values are only nonzero if the corresponding half-edge types have a nonzero probability to occur simultaneously on the same nodes. Thus, only the following values contribute:

$$\begin{aligned} \mathbb{E}[k_{2g-1}k_{2g}] &= \mu_{11}^{[g]} n(g), \\ \mathbb{E}\left[k_{2g-1}^2\right] &= \mu_{20}^{[g]} n(g), \\ \mathbb{E}\left[k_{2g}^2\right] &= \mu_{02}^{[g]} n(g). \end{aligned} \tag{14}$$

The expectation values for any other combinations of half-edge types in $\mathbb{E}[k_ik_j]$ are equal to zero. By combining the expressions for $\mathbb{E}[k_j]$ and $\mathbb{E}[k_ik_j]$ and using Eq. (7), we simplify Eq. (10) to

$$\boldsymbol{M} = \begin{pmatrix} \boldsymbol{C}^{[1]} & \mathbf{0} & \cdots & \mathbf{0} \\ \mathbf{0} & \boldsymbol{C}^{[2]} & \ddots & \vdots \\ \vdots & \ddots & \ddots & \mathbf{0} \\ \mathbf{0} & \cdots & \mathbf{0} & \boldsymbol{C}^{[G]} \end{pmatrix}. \tag{15}$$

The 2×2 block matrices $\boldsymbol{C}^{[g]}$ are of shape

$$\boldsymbol{C}^{[g]} = \lambda \begin{pmatrix} P(g) & P(g) \\ Q(g) & Q(g) \end{pmatrix}, \tag{16}$$

where

$$\lambda = \frac{\mu_2 - \mu_1}{\mu_1} \tag{17}$$

does not depend on the generation $g \in \{2, \ldots, G-1\}$.

1. Percolation threshold of the generation model

If a colored graph satisfies degree distribution $u(\boldsymbol{k})$, the degree distribution after removal of a p fraction of edges uniformly at random is written as [26]

$$u'(\boldsymbol{k}') = \sum_{\boldsymbol{k}\geqslant 0} \prod_{i=1}^{2G} \binom{k_i}{k_i'} p^{k_i'}(1-p)^{k_i - k_i'} u(\boldsymbol{k}). \tag{18}$$

The expectation values of $u(\boldsymbol{k})$ and $u'(\boldsymbol{k}')$ are related as

$$\begin{aligned} \mathbb{E}[k_i'] &= p\mathbb{E}[k_i], \\ \mathbb{E}[k_i'k_j'] &= p^2\mathbb{E}[k_ik_j] + (p - p^2)\mathbb{E}[k_i]\delta_{i,j} \end{aligned} \tag{19}$$

and the percolation threshold corresponds to the percolation parameter p, for which the system exhibits criticality. At criticality, the component size distribution shows scale-free behavior, which is fulfilled if and only if

$$\boldsymbol{P}\boldsymbol{M}'\boldsymbol{v} = \boldsymbol{v}, \tag{20}$$

where $\boldsymbol{v}$ has all elements positive and the matrix $\boldsymbol{M}'$ is solely characterized by the expectation values of an arbitrary degree distribution $u'(\boldsymbol{k}')$ according to Eq. (10). The derivation of Eq. (20) can be found in Ref. [26].

Substituting Eq. (19) into Eq. (10) results in $\boldsymbol{M}' = p\boldsymbol{M}$. In the directed m-colored random graph [26], the percolation threshold is given by the solution to the eigenvalue problem

$$\boldsymbol{P}\boldsymbol{M}\boldsymbol{v} = \lambda\boldsymbol{v}, \quad \text{with } \lambda = \frac{1}{p_{\text{crit}}}, \tag{21}$$

for the critical percolation threshold.

Now we show that the largest eigenvalue of $\boldsymbol{P}\boldsymbol{M}$ in the special case of the generation model with $\boldsymbol{P}$ and $\boldsymbol{M}$ according to Eqs. (9) and (15) is given by $\lambda = \frac{\mu_2 - \mu_1}{\mu_1}$. By a simple check one can see that the vector $\mathbf{v} = (1, 1, \ldots, 1)$ is a left eigenvector of $\boldsymbol{M}$:

$$\mathbf{v}\boldsymbol{M} = \lambda\mathbf{v}. \tag{22}$$

Since all elements of $\mathbf{v}$ are the same and $\boldsymbol{P}$ is a permutation matrix, one may substitute $\mathbf{v}\boldsymbol{P} = \mathbf{v}$ to obtain $\mathbf{v}\boldsymbol{P}\boldsymbol{M} = \lambda\mathbf{v}$, and therefore $\boldsymbol{P}\boldsymbol{M}$ has an eigenvalue λ.

Due to its special shape, $\boldsymbol{M}$ can be rewritten as $\boldsymbol{M} = \lambda\boldsymbol{D}\boldsymbol{B}$, with the diagonal matrix $\boldsymbol{D} = \text{diag}(P(1), Q(1), \ldots, P(G), Q(G))$ and the block diagonal matrix $\boldsymbol{B} = \text{diag}(\boldsymbol{J}_1, \ldots, \boldsymbol{J}_G)$ with $\boldsymbol{J}_i = \boldsymbol{J}$ for $i = 1, \ldots, G$ and $\boldsymbol{J}$ being a 2×2 all-ones matrix. We will now show that λ is the largest eigenvalue, or the spectral radius of $\boldsymbol{P}\boldsymbol{M}$. Due to Gelfand's formula, the spectral radius of the matrix product is bounded by $\rho(\boldsymbol{P}\boldsymbol{M}) = \rho(\lambda\boldsymbol{P}\boldsymbol{D}\boldsymbol{B}) \leqslant \lambda\rho(\boldsymbol{P})\rho(\boldsymbol{D})\rho(\boldsymbol{B}) \leqslant \lambda$, as $\rho(\boldsymbol{P}) = \rho(\boldsymbol{B}) = 1$ and $\rho(\boldsymbol{D}) \leqslant 1$. The eigenvalue λ coincides with a known upper bound on the eigenvalue spectrum. Therefore, for an arbitrary volume growth function, the critical percolation probability $p_{\text{crit}} = \frac{1}{\lambda}$ of the network is given by

$$p_{\text{crit}} = \frac{\mu_1}{\mu_2 - \mu_1}. \tag{23}$$

This expression coincides with the critical percolation probability for an undirected unicolored random graph [29] and degree distribution $u(k)$.

2. Percolation threshold with intrageneration edges

Until now we have only considered edges that connect two consecutive generations, which led to the pairing rules defined by the permutation matrix in Eq. (9). In this section we will also allow edges within one generation, as illustrated in Fig. 2. Let us introduce the parameter a that defines the probability that a half-edge of any given type connects to a half-edge of

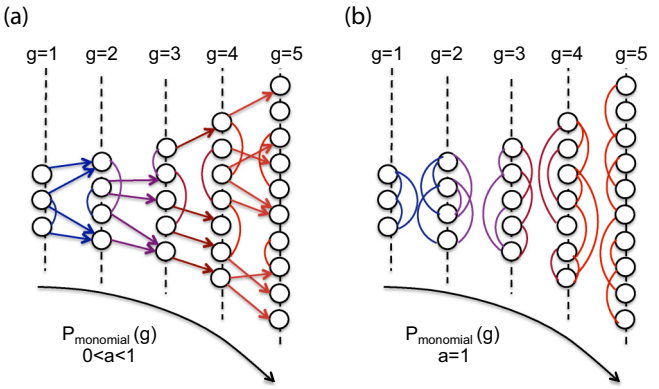

FIG. 2. Illustration of the generation model with intrageneration edges. The intrageneration edges are represented by undirected edges. Two networks with different fractions of intrageneration edges are presented: (a) $0 < a < 1$, leading to the coexistence of directed edges that connect consecutive generations and undirected edges within one generation, and (b) $a = 1$, leading to a network with the generations being disconnected.

the same type. This leads to the permutation matrix

$$\tilde{\boldsymbol{P}} = \begin{pmatrix} a & 0 & 0 & 0 & 0 & 1-a \\ 0 & \tilde{\boldsymbol{P}}^{[1]} & \boldsymbol{0} & \cdots & \boldsymbol{0} & 0 \\ 0 & \boldsymbol{0} & \tilde{\boldsymbol{P}}^{[1]} & \ddots & \vdots & \vdots \\ \vdots & \vdots & \ddots & \ddots & \boldsymbol{0} & 0 \\ 0 & \boldsymbol{0} & \cdots & \boldsymbol{0} & \tilde{\boldsymbol{P}}^{[1]} & 0 \\ 1-a & 0 & 0 & 0 & 0 & a \end{pmatrix}, \tag{24}$$

with

$$\tilde{\boldsymbol{P}}^{[1]} = \begin{pmatrix} a & 1-a \\ 1-a & a \end{pmatrix}. \tag{25}$$

In a similar manner as in the preceding section we prove that the parameter a does not affect the percolation threshold. First, it can easily be shown that the equality $\mathbf{v}\tilde{\boldsymbol{P}} = \mathbf{v}$ still holds. Second, as the matrix $\boldsymbol{M}$ is not affected, the spectral radius is again bounded by $\rho(\tilde{\boldsymbol{P}}\boldsymbol{M}) = \rho(\lambda\tilde{\boldsymbol{P}}\boldsymbol{D}\boldsymbol{B}) \leqslant \lambda\rho(\tilde{\boldsymbol{P}})\rho(\boldsymbol{D})\rho(\boldsymbol{B})$, with $\rho(\boldsymbol{B}) = 1$ and $\rho(\boldsymbol{D}) \leqslant 1$. As $\tilde{\boldsymbol{P}}$ is the product of a permutation matrix and the block diagonal matrix $\mathrm{diag}(\tilde{\boldsymbol{P}}^{[1]}, \ldots, \tilde{\boldsymbol{P}}^{[1]})$ of dimensions $2G \times 2G$, its distinct eigenvalues are given by the eigenvalues of $\tilde{\boldsymbol{P}}^{[1]}$, that is, $\tilde{\lambda} = a \pm (a-1)^2$. Given that $a \in [0, 1]$, the eigenvalues are bounded by $\tilde{\lambda} = \pm 1$, which bounds the spectral radius to $\rho(\tilde{\boldsymbol{P}}) \leqslant 1$. Thus, $\rho(\boldsymbol{P}\boldsymbol{M}) \leqslant \lambda$ and Eq. (23) still holds for $\lambda = \frac{\mu_2 - \mu_1}{\mu_1}$.

Even though the percolation threshold remains invariant when allowing for edges within one generation, the network structure changes drastically. While for $a = 0$ the system simplifies to the previously discussed case of no edges within one generation and a fully directed acyclic graph, $0 < a < 1$ corresponds to a system with both directed edges connecting consecutive generations and undirected edges within one generation present, as shown in Fig. 2(a). The extreme case of $a = 1$ defines a system where all generations become disconnected [see Fig. 2(b)]. While separated from other generations, every generation on its own is equivalent to a bicolored undirected random graph characterized by the permutation matrix

$$\tilde{\boldsymbol{P}}^{[1]}_{a=1} = \begin{pmatrix} 1 & 0 \\ 0 & 1 \end{pmatrix}, \tag{26}$$

which exhibits the same percolation threshold as the global system.

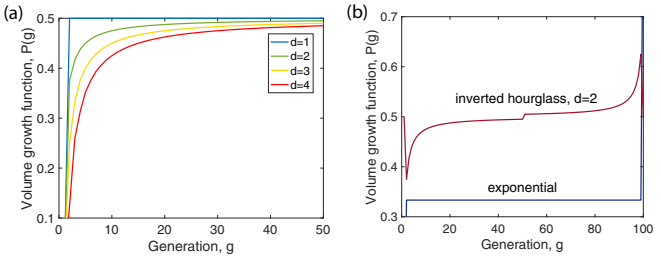

FIG. 3. Various volume growth functions $P(g)$: (a) monomial growth with dimensionality $d = 1, 2, 3, 4$ and (b) exponential growth with $\alpha = 2$ and inverted hourglass with $d = 2$.

B. Examples of volume growth functions

In the following section we will discuss examples of the volume growth function $P(g)$. The growth function can be chosen fully arbitrarily, as long as it fulfills the following conditions: (a) $[1 - P(g)]n(g) = P(g+1)n(g+1)$, as defined in Eq. (1); (b) $0 \leqslant P(g) \leqslant 1$ for all $g \in \{1, \ldots, G\}$; (c) $P(1)n(1) = [1 - P(G)]n(G)$ with $n(G)$ in accordance with Eq. (2); and (d) $P(g) > 0$ for at least one $g \in \{1, \ldots, G\}$. If one of the first three constraints is violated, the network does not satisfy the degree distribution $u(k)$, and $n(g) = 0$ for all $g \in \{1, \ldots, G\}$ in case of the violation of the fourth condition. If the system is chosen such that no edges exist between the first and last generation, meaning $P(1) = 0$ and $P(G) = 1$, the third condition is trivial. If the number of edges between the first and last generation is chosen to be nonzero, one simple scenario is $n(1) = n(G)$, which leads to the conditions $P(1) = 1 - P(G)$. In this section, only these two scenarios will be considered.

We will discuss three types of volume growth: (i) exponential growth with $n(g) \propto \alpha^g$, (ii) monomial growth with $n(g) \propto g^{d-1}$, and (iii) the inverted hourglass. In the case of the inverted hourglass, we connect the first and last generations, whereas in (i) and (ii) we do not connect them. In Fig. 3, $P(g)$ is illustrated for all three types of volume growth.

The volume growth function featuring an exponential increase of the fraction of nodes with generations is the simplest case. The dependence $n(g) \propto \alpha^g$ is achieved by defining the volume growth function as

$$P_{\mathrm{exponential}}(g) = \begin{cases} 0 & \text{for } g = 1 \\ \frac{1}{\alpha+1} & \text{for } 1 < g < G \\ 1 & \text{for } g = G. \end{cases} \tag{27}$$

If $\alpha = 1$, the number of nodes is constant for any generation. No edges connecting the first and last generations are present.

In order to ensure monomial behavior in the number of nodes per generation, we relate the expected number of nodes in generation g, $n(g)$, to the surface area of a ball at radius r with radius $r = g\Delta r$, with the incremental radius $\Delta r > 0$ and

the dimensionality d. Thus, the ratio of the number of nodes of two consecutive generations is proportional to the ratio of the surface area of a ball at radius $r + \Delta r$ to the surface area of a ball with radius r, $\frac{n(g+1)}{n(g)} = \frac{(r+\Delta r)^{d-1}}{r^{d-1}}$, or equivalently

$$x(g) = \left(1 + \frac{1}{g}\right)^{d-1}. \tag{28}$$

In the one-dimensional case $d = 1$, $n(g)$ is constant over all generations. For $d \geqslant 2$, $n(g)$ increases proportionally to g^{d-1}. The volume growth function $P(g)$ is then given by

$$P_{\text{monomial}}(g) = \begin{cases} 0 & \text{for } g = 1 \\ P(2) & \text{for } g = 2 \\ P(g) = \frac{1-P(g-1)}{x(g-1)} & \text{for } 3 \leqslant g \leqslant G \\ 1 & \text{for } g = G. \end{cases} \tag{29}$$

Here $P(2)$ is chosen such that the function $P(g)$ is stable, which is the case for

$$P(2) = \begin{cases} \frac{1}{2} & \text{for } d = 1 \\ \frac{3}{8} & \text{for } d = 2 \\ \frac{1}{x(1)} & \text{for } d \geqslant 3. \end{cases} \tag{30}$$

In the case of the inverted hourglass, any volume growth function $P(g)$ that causes an increase in the nodes followed by an decrease can be chosen. For simplicity, we define a symmetric growth by

$$P_{\text{hourglass}}(g) = \begin{cases} \frac{1}{2} & \text{for } g = 1 \\ P(g) & \text{for } 1 < g < \frac{G}{2} \\ \frac{1}{2} & \text{for } g = \frac{G+1}{2} \text{ if } G \text{ odd} \\ 1 - P(G-g) & \text{for } \frac{G}{2} < g < G \\ \frac{1}{2} & \text{for } g = G. \end{cases} \tag{31}$$

For monomial growth $P(g) = P_{\text{monomial}}(g)$ with dimensionality d as depicted in Fig. 3(b). Depending on the choice of $P(g)$, $P_{\text{hourglass}}(g)$ exhibits the shape of an hourglass or inverted hourglass.

III. RESULTS

In this section we compare results of the analytic predictions of the theory to stochastic simulations for various global properties of the generation model. Stochastic simulations allow us to recover various global properties of the network from the adjacency matrix $\boldsymbol{A}$, e.g., the largest component, the percolation threshold, the cyclomatic number, the node neighborhood size, and the average shortest path. For simplicity, in the current section only regular graphs with functionality F are considered, i.e., systems that satisfy the degree distribution $u(k)$ with $u(F) = 1$ and $u(k) = 0$ otherwise.

In Fig. 4, generated regular graphs with $F = 3$ and various volume growth functions are studied. The shown topologies depict the spanning tree of the full network, i.e., no cycles are depicted in the illustration. Figure 4(a i) illustrates the unicolored random graph without generations exhibiting a different topology with edges being highly stretched when embedded in the Euclidean two-dimensional plane with the ForceAtlas algorithm. Figures 4(a ii)–4(a iv) show generated network topologies with monomial volume growth $P_{\text{monomial}}(g)$ with $d = 1, 2, 3$. The color gradient from blue to red indicates increasing generations. For $d = 1$, the obtained topology resembles a snakelike structure with the number of nodes per generation fluctuating around a constant and the number of nodes in the first generation $n(1) = 20$. For $d = 2$, the topology uniformly fills the two-dimensional plane. For $d = 3$, the nodes become more crowded on the plane with increasing generations forming a boundary.

The neighborhood size is the cumulative sum of the number of ith-order neighbors around a reference node. This quantity describes the local volume growth behavior as a function of a distance to a uniformly selected reference node. One observes a crossover between different behavior of the volume growth function for the small and large distances. Figure 4(b) reports the number of nodes at a distance less than or equal to the one given for a generated network with $F = 3$. As the measure of distance we use the undirected shortest path between two given nodes, which is the shortest path irrespective of the orientation of the edges. In Figs. 4(b ii)–4(b iv) the observed neighborhood size grows monomially with the shortest path, in line with the underlying volume growth function in the generation model that imposes (ii) one-dimensional, (iii) two-dimensional, and (iv) three-dimensional growth. Figure 4(b i) illustrates the same quantity for the regular network without generations, which exhibits exponential growth. In the case of one-dimensional monomial growth, deviations from the expected neighborhood growth are observed for small l, which are explained as follows. Initially, the neighborhood of a node grows exponentially with $V(l) \propto \alpha^l$, with $\alpha = F - 1$. Once the neighborhood size $V(l)$ of a node in generation g is similar to that of the expected number of nodes in the generation $n(g)$, the growth behavior changes from the exponential growth to the one imposed by the growth function. The one-dimensional network is obtained from a generation network with $n(1) = 50$, whereas the two- and three-dimensional networks are obtained from the generation networks with $n(1) = 5$ and $n(1) = 1$, respectively.

Figure 4(c) illustrates the neighborhood sizes for nodes that lie in higher generations. Here all subplots exhibit initial exponential growth, which eventually changes to monomial growth for the networks with monomial volume growth function. In the case of $d = 3$, the regime with monomial growth behavior is relatively short due the finite size of the stochastic network. The behavior of the neighborhood size of the regular network without generations as shown in Figs. 4(b i) and 4(c i) is identical, as the nodes in the network are indistinguishable.

Figure 5 illustrates the average shortest path of all pairs of nodes for networks with distinct volume growth functions. The data points are obtained for five independent networks for every volume growth function. Small-world networks exhibit $\langle l \rangle \propto \log(N)$ behavior, whereas the average shortest path in spatial networks with monomial growth exhibits $\langle l \rangle \propto N^{1/d}$ behavior. For small system sizes we observe that the studied networks exhibit $\langle l \rangle \propto \log(N)$ growth. However, for larger systems the behavior switches to $\langle l \rangle \propto N^{1/d}$ for $d = 1, 2$. For $d = 3$, it is not clear if an actual change in the slope is observed or if the considered system size is still too small.

Figure 6 illustrates percolated networks with the functionalities $F = 3, 4, 5$, monomial growth $d = 1, 2, 3$, and the total number of nodes $N = 20\,000$. Figure 6(a) shows that

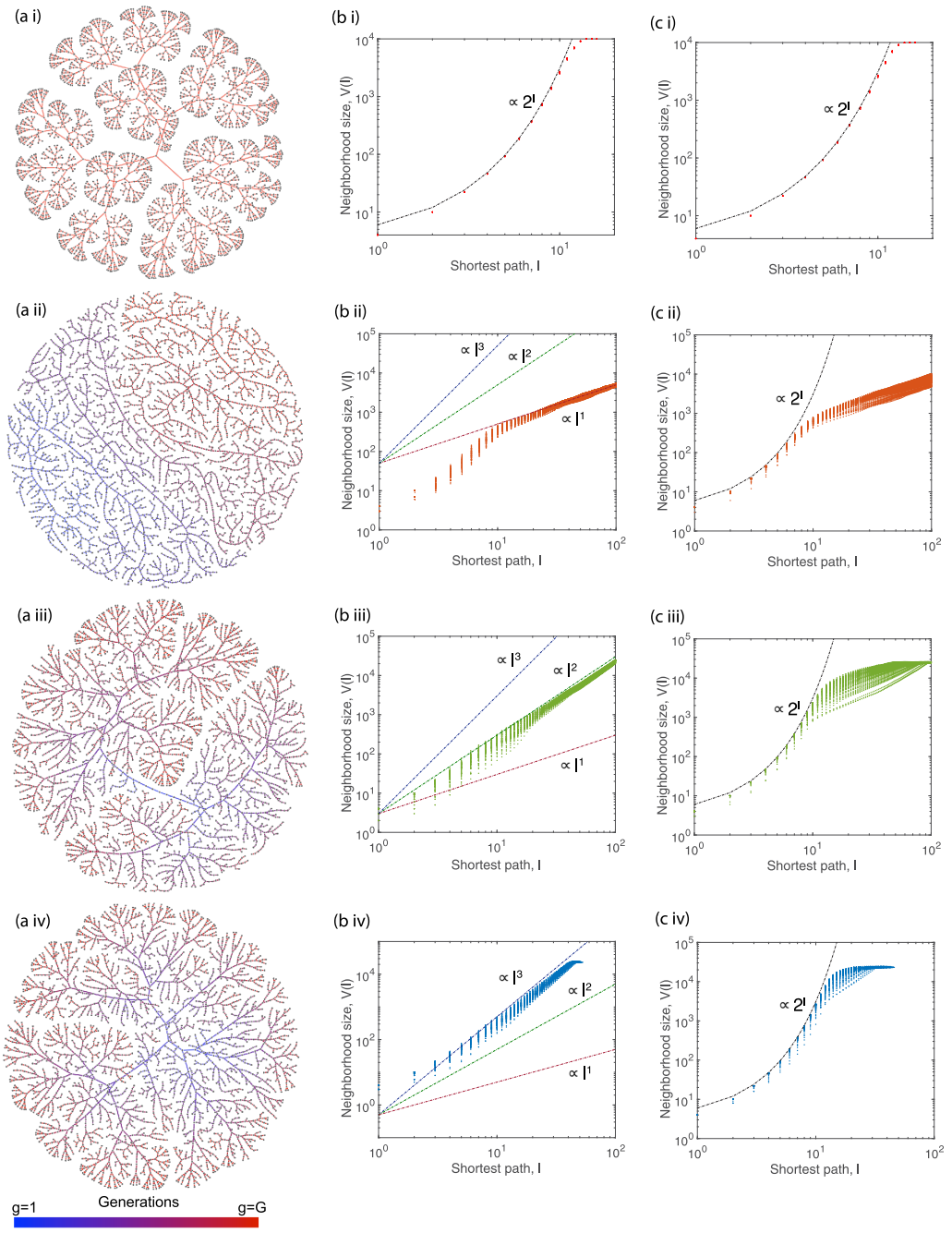

FIG. 4. Regular networks with degree $F = 3$ (no cycles) with various types of growth behavior: (i) exponential growth, (ii) one-dimensional monomial growth, (iii) two-dimensional monomial growth, and (iv) three-dimensional monomial growth. (a) Spanning trees (no cycles). The color gradient indicates the generations. (b) and (c) Node neighborhood size $V(l)$ with shortest path l for (b) nodes in first generations and (c) nodes in higher generations. The data (dots) are obtained from stochastic generation networks of size $N = 20\,000$. The dash-dotted lines in (b ii)–(b iv) illustrate the expected neighborhood size for monomial growth and in (b i) and (c i)–(c iv) the expected neighborhood size for exponential growth. In (c ii)–(c iv) the neighborhood first growths exponentially until it switches to monomial growth independent of the volume growth function.

for all considered F the normalized sizes of the largest components collapse to one line for various d. This figure confirms the proof in Sec. II A 2 that the percolation threshold of the generation model with degree distribution $u(\boldsymbol{k})$ indeed coincides with the percolation threshold of the random graph with the corresponding monovariate degree distribution $u(k)$ with $k = \sum_{i=1}^{2G} k_i$. Moreover, we observe that also the relative largest-component sizes coincide with the predicted giant-component size for the random regular graph. Only close to the transition point p_{crit} we notice small deviations, which are most probably due to finite-size effects.

In Fig. 6(b) the normalized cyclomatic number of the largest component (circles) obtained from the stochastic

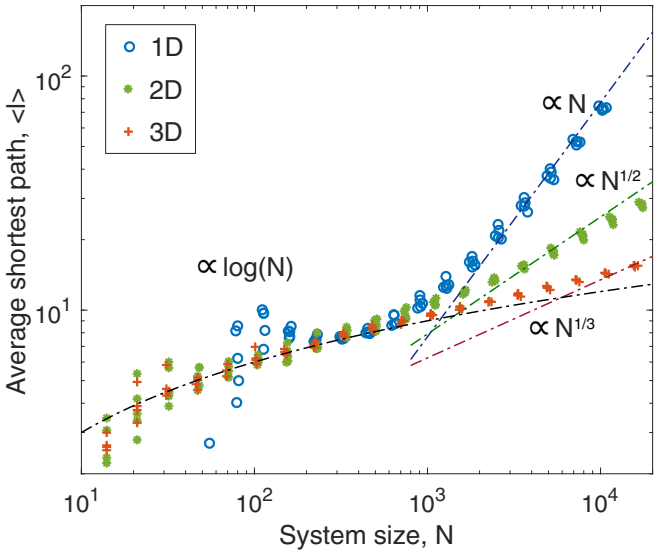

FIG. 5. Average shortest path as a function of system size for regular networks with degree $F = 3$. Networks with different volume growth functions are studied: one dimensional (circles), two dimensional (stars), and three dimensional (crosses). The dash-dotted lines indicate the expected growth of the average path.

simulation is illustrated for $F = 3, 4, 5$ and $d = 1, 2, 3$. The normalized cyclomatic number is a measure for the fraction of edges that can be removed without breaking the network. The observations from generated networks are in good agreement with the theoretical predictions of the normalized cyclomatic number of the giant component.

IV. CONCLUSION

Spatial networks exhibit a variety of peculiar properties such as clustering, sparsity, degree-degree correlations, volume growth, and percolation thresholds. It is not clear if biasing or constraining a random network to reproduce one of these features would imply emergence of the other. One of the most characteristic properties of spatial networks is that their volume scaling is related to the underlying metrical space. The other peculiarity is that the percolation thresholds in spatial networks tend to be larger than the threshold in the configuration model with the same degree sequence. In this paper we asked the following question: Is the delay of the percolation threshold observed in spatial networks related to the volume growth function of the underlying space or it is a consequence of other network properties that occur in spatial networks? The answer is negative: We proved analytically and demonstrated in numerical experiments that for a G-layered network with a given degree distribution neither the volume growth function nor the number of generations has an effect on the percolation threshold.

These findings contribute to the long-standing discussion on the effect of volume growth on the network's topology. An earlier study by Eichinger [2] proposed a model with a substantial shift in the percolation threshold due to the monomial volume growth, to the extent that no percolation was observed for random regular graphs with $F = 3$. The model did not consider weakly connected components, i.e.,

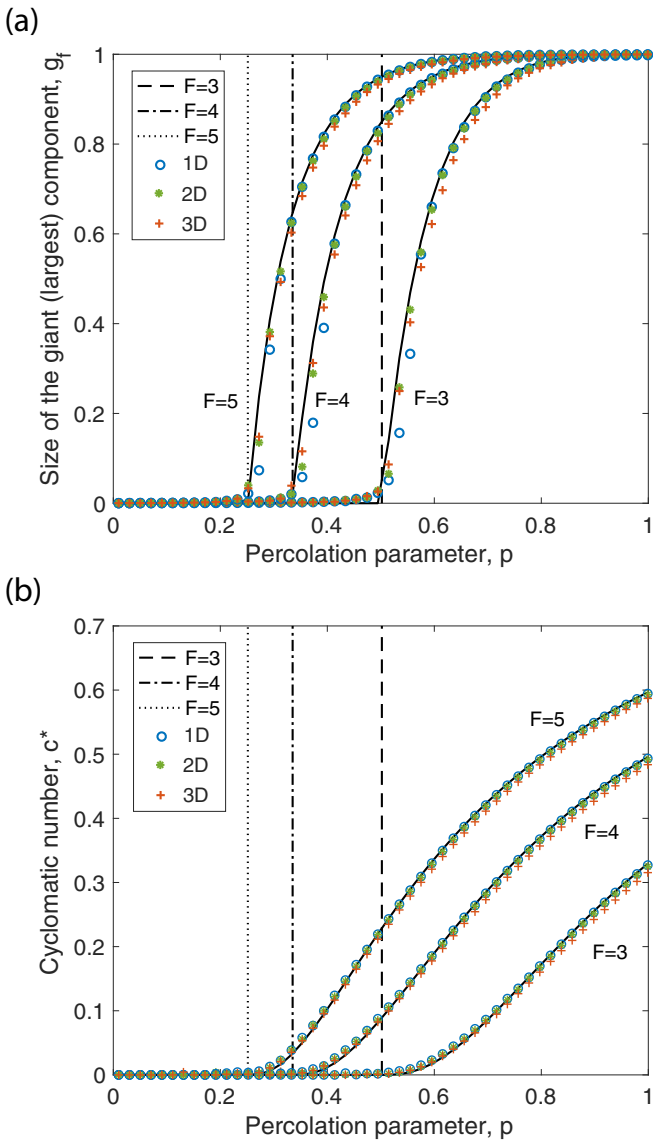

FIG. 6. Percolation on regular graphs with various types of monomial growth behavior with functionalities $F = 3, 4, 5$: (a) size of the largest or giant component and (b) cyclomatic number. The different types of growth behavior are indicated by markers: one dimensional (circles), two dimensional (stars), and three dimensional (crosses). The percolation points for the different functionalities are indicated by the dashed, dash-dotted, and dotted line for $F = 3, 4, 5$, respectively. The data points are obtained from networks of size $N = 20\,000$ and compared to the percolation on a random regular graph (solid lines).

all connected components had one distinct root node that is connected to every node of the connected component by a directed path. The present paper dissolves this restriction by allowing weak connectivity and thus an arbitrary number of root nodes of one connected component.

The presented findings shed light on at least one of the reasons why the Molloy-Reed criterion [37,38] and the configuration model predict the percolation threshold reasonably well even for networks with nonexponential volume growth, such as the polymer networks [1,10]. This indicates that predicting emergent properties of real-world networks does

not necessarily require network models to satisfy a consistent volume growth function and therefore extends the number of application areas for simple network models, such as the configuration model, especially in the field of polymer science.

It is important to note that we only studied the emergent properties under volume growth in a maximum entropy graph with given degree distribution. We did not study the effect of volume growth in the presence of other topological features such as degree-degree correlations or clustering, which are known to strongly alter the percolation threshold. Furthermore, as volume growth and other topological features might interfere, they cannot be studied separately. The combined effects of the volume growth and local topological features still need extensive study and we hope that this work will encourage the exploration of such effects more thoroughly in the future.

It is noteworthy that the discussed network model characterizes an infinite random directed acyclic graph. Thus, it has high potential to be utilized in the research fields of directed acyclic graphs in the future.

ACKNOWLEDGMENTS

This research was supported by Océ Technologies B.V. and the Technology Foundation STW. I.K. acknowledges support from research program Veni, Project No. 639.071.511, which is financed by the NWO.

APPENDIX A: STOCHASTIC SIMULATION

In order to test the theoretical predictions, we developed a stochastic algorithm for generating samples of random networks with a given growth function and degree distribution. In the simulation, the network is constructed generation by generation in a consecutive manner. Here we only consider network without edges between the last and first generations, meaning that $P(1) = 1 - P(G) = 0$. Starting at generation $g = 1$, the number of nodes is given by $n(1)N$. The number of out-edges for every node in the first generation is sampled from the degree distribution $u^{[1]}(0, k) = u(k)$. The out-edges are than partitioned into sets of $k_1 = 1, 2, 3, \ldots$ edges according to the probability distribution $\sum_{k_2} u^{[2]}(k_1, k_2)$. The number of sets defines the number of nodes in generation $g = 2$, $n(2)$, and the sets themselves define the number of in-edges for every node. Having the nodes of generation $g = 2$ and their in-edges in hand, the number of out-edges for the nodes is drawn from $u^{[g]}(k_1, k_2)$, in this case with $g = 2$, k_1 being the number of in-edges of the individual node.

The topology of the network is stored as an adjacency matrix $\boldsymbol{A}$. All nodes are assigned indices. An edge between node n_1 in generation g and node n_2 in generation $g + 1$ is recorded as $A(n_1, n_2) = g$, and $A(n_1, n_2) = 0$ if no edge is present. In this way the information on the generation of origin and the orientation of the edge is stored. The process of percolation is studied by randomly deleting nonzero elements of $\boldsymbol{A}$ with probability $1 - p$, with p the percolation parameter, and monitoring the size of the largest component.

In a finite system, the cyclomatic number is defined as the maximum number of edges that can be removed from a network without breaking it. It is defined as

$$c = e - n + z, \tag{A1}$$

with e the number of edges, n the number of nodes, and z the number of components. We define the normalized cyclomatic number of the largest component as

$$c^* = \frac{c}{e} = 1 - \frac{n}{e} + \frac{1}{e}, \tag{A2}$$

with e the number of edges and c the cyclomatic number of the largest component, and $z = 1$.

APPENDIX B: UNDIRECTED UNICOLORED RANDOM GRAPH WITH ARBITRARY DEGREE DISTRIBUTION: PERCOLATION, GIANT COMPONENT, AND CYCLOMATIC NUMBER

This Appendix gives a brief summery of the undirected random graph with arbitrary degree distribution [39], as we derive an expression for the cyclomatic number from this theory. This random graph, only constrained by the degree distribution, is equivalent to the configuration model in the thermodynamic limit ($N \to \infty$). We discuss the size of the giant component g_f, the probability of an edge being part of the giant component g_f^{edges}, and the derived normalized cyclomatic number c^*.

The random graph satisfies an arbitrary one-variate degree distribution $u(k)$ with the node degree $k \in \{0, 1, 2, \ldots\}$. The moments of the degree distribution are defined according to Eq. (4). The percolation process on the random graph is equivalent to the random removal of edges with probability $1 - p$ or an edge being present with probability p, respectively. The probability p is referred to as the percolation parameter. Thus, the degree distribution with percolation is described by the binomial distribution

$$u'(k') = \sum_{k \geqslant 0} \binom{k}{k'} p^k (1-p)^{k-k'} u(k). \tag{B1}$$

Any property derived from the arbitrary degree distribution $u(k)$ can also be derived from the percolation degree distribution $u'(k')$.

In order to derive the size of the giant component, we introduce the generating function of the degree distribution as

$$U(x) = \sum_{k \geqslant 0} x^k u(k). \tag{B2}$$

Let us define the generating function of the excess degree distribution as

$$U_1(x) = \frac{1}{\mu_1} \frac{d}{dx} U(x), \tag{B3}$$

with μ_1 the first moment of the degree distribution. Solving the system of equations

$$\begin{aligned} W_1(x) &= U_1(W_1(x)), \\ W(x) &= U(W_1(x)), \end{aligned} \tag{B4}$$

we obtain the size of the giant component by

$$g_f^{\text{nodes}} = 1 - W(1). \tag{B5}$$

The normalized size of the giant component is equivalent to the probability of a node to be part of the giant component. In order for an edge to be part of the giant component, it has to be connected to the giant component only on its right end, only on its left end, or on both ends. The probability of an edge to be connected to the giant component on its right end is given by $p_{gc} = 1 - W_1(1)$, which is equal to the probability to be connected on it left end. Thus, the probability that the edges is connected to the giant component at least on one of its ends is given by $g_f^{\text{edges}} = 2p_{gc}(1 - p_{gc}) + p_{gc}^2$, which simplifies to

$$g_f^{\text{edges}} = 1 - W_1(1)^2. \tag{B6}$$

In infinite networks, the normalized cyclomatic number of the giant component is defined as the fraction of edges that can be removed from the giant component without breaking it. As the systems size is infinite and thus also the number of edges, the term $\frac{1}{e}$ of Eq. (A2) vanishes. The second term $\frac{n}{e}$ is rewritten as

$$\frac{n}{e} = \frac{\frac{n}{N}}{\frac{e}{E}\frac{E}{N}}, \tag{B7}$$

with

$$\frac{n}{N} = g_f, \quad \frac{e}{E} = g_f^{\text{edges}}, \quad \frac{E}{N} = \frac{1}{2}\mu_1. \tag{B8}$$

The expressions $\frac{n}{N}$ and $\frac{e}{E}$ denote, respectively, the node and edge fractions of the system that are part of the giant component and $\frac{E}{N}$ is the ratio of edges versus nodes in the system. The following definitions are introduced: g_f denotes the size fraction of the giant component, g_f^{edges} defines the fraction of edges of the system that are part of the giant component as given in Eq. (B6), and μ_1 is the expected degree according to Eq. (4). Thus, the normalized cyclomatic number of the giant component is given as

$$c^* = \frac{c}{e} = 1 - \frac{g_f}{\frac{1}{2}\mu_1 g_f^{\text{edges}}}. \tag{B9}$$

[1] V. Schamboeck, P. D. Iedema, and I. Kryven, Sci. Rep. **9**, 2276 (2019).
[2] B. Eichinger, Polymer **46**, 4258 (2005).
[3] F.-B. Mocnik, Sci. Rep. **8**, 11274 (2018).
[4] L. Daqing, K. Kosmidis, A. Bunde, and S. Havlin, Nat. Phys. **7**, 481 (2011).
[5] D. Li, G. Li, K. Kosmidis, H. Stanley, A. Bunde, and S. Havlin, Europhys. Lett. **93**, 68004 (2011).
[6] T. Emmerich, A. Bunde, S. Havlin, G. Li, and D. Li, Phys. Rev. E **87**, 032802 (2013).
[7] A. P. Kartun-Giles, M. Barthelemy, and C. P. Dettmann, Phys. Rev. E **100**, 032315 (2019).
[8] V. Schamboeck, I. Kryven, and P. D. Iedema, Macromol. Theory Simul. **26**, 1700047 (2017).
[9] I. Kryven and P. D. Iedema, Chem. Eng. Sci. **126**, 296 (2015).
[10] A. Torres-Knoop, I. Kryven, V. Schamboeck, and P. D. Iedema, Soft Matter **14**, 3404 (2018).
[11] N. Alalwan, A. Arenas, and E. Estrada, J. Math. Chem. **57**, 875 (2019).
[12] L. Speidel, H. A. Harrington, S. J. Chapman, and M. A. Porter, Phys. Rev. E **98**, 012318 (2018).
[13] D. Krioukov, F. Papadopoulos, M. Kitsak, A. Vahdat, and M. Boguná, Phys. Rev. E **82**, 036106 (2010).
[14] M. Barthelemy, *Morphogenesis of Spatial Networks* (Springer, Berlin, 2018).
[15] M. A. Serrano, D. Krioukov, and M. Boguná, Phys. Rev. Lett. **100**, 078701 (2008).
[16] G. Bianconi and C. Rahmede, Sci. Rep. **7**, 41974 (2017).
[17] D. C. da Silva, G. Bianconi, R. A. da Costa, S. N. Dorogovtsev, and J. F. F. Mendes, Phys. Rev. E **97**, 032316 (2018).
[18] A. Faqeeh, S. Osat, and F. Radicchi, Phys. Rev. Lett. **121**, 098301 (2018).
[19] S. Lämmer, B. Gehlsen, and D. Helbing, Physica A **363**, 89 (2006).
[20] R. Guimera, S. Mossa, A. Turtschi, and L. N. Amaral, Proc. Natl. Acad. Sci. USA **102**, 7794 (2005).
[21] N. Cressie, J. Frey, B. Harch, and M. Smith, J. Agr. Biol. Envir. Stat. **11**, 127 (2006).
[22] P. Skehan and S. J. Friedman, Cell Proliferat. **17**, 335 (1984).
[23] J. Li, M. Dao, C. Lim, and S. Suresh, Biophys. J. **88**, 3707 (2005).
[24] D. B. Taylor, H. S. Dhillon, T. D. Novlan, and J. G. Andrews, *2012 IEEE Global Communications Conference (GLOBECOM)* (IEEE, Piscataway, 2012), pp. 4524–4529.
[25] M. Boguna, D. Krioukov, P. Almagro, and M. Serrano, arXiv:1909.00226.
[26] I. Kryven, Nat. Commun. **10**, 404 (2019).
[27] A. P. Kartun-Giles and G. Bianconi, Chaos Soliton. Fractal: X **1**, 100004 (2019).
[28] I. Erukhimovich, M. V. Thamm, and A. V. Ermoshkin, Macromolecules **34**, 5653 (2001).
[29] I. Kryven, J. Math. Chem. **56**, 140 (2018).
[30] A. Bunde, S. Havlin, and M. Porto, Phys. Rev. Lett. **74**, 2714 (1995).
[31] B. Karrer and M. E. J. Newman, Phys. Rev. E **80**, 046110 (2009).
[32] J. R. Clough, J. Gollings, T. V. Loach, and T. S. Evans, J. Complex Netw. **3**, 189 (2015).
[33] I. Shrier and R. W. Platt, BMC Med. Res. Methodol. **8**, 70 (2008).
[34] T. J. VanderWeele and J. M. Robins, Epidemiology **18**, 561 (2007).
[35] S. Allesina and A. Bodini, Ecol. Complex. **2**, 323 (2005).
[36] I. Kryven, Phys. Rev. E **96**, 052304 (2017).
[37] S. Melnik, A. Hackett, M. A. Porter, P. J. Mucha, and J. P. Gleeson, Phys. Rev. E **83**, 036112 (2011).
[38] M. Molloy and B. Reed, Random Struct. Algor. **6**, 161 (1995).
[39] M. E. J. Newman, S. H. Strogatz, and D. J. Watts, Phys. Rev. E **64**, 026118 (2001).